Section: Neurobiology of Disease

The Periodontium Damage Induces Neuronal Cell Death in the Trigeminal Mesencephalic Nucleus and Neurodegeneration in the Trigeminal Motor Nucleus in C57BL/6J Mice

Ashis Dhar[1], Eriko Kuramoto[1], Makoto Fukushima[1], Haruki Iwai[1], Atsushi Yamanaka[1], Tetsuya Goto[1]

[1]Division of Oral Anatomy and Cell Biology, Kagoshima University Graduate School of Medical and Dental Science, 8-35-1 Sakuragaoka, Kagoshima 890-8544, Japan

E-mail: Ashis Dhar: k3774330@kadai.jp

Eriko Kuramoto: kuramoto@dent.kagoshima-u.ac.jp

Makoto Fukushima: k5239286@kadai.jp

Haruki Iwai: haruki@dent.kagoshima-u.ac.jp

Atsushi Yamanaka: yamanaka@dent.kagoshima-u.ac.jp

Running title: Neurodegeneration of Vmes and Vmo nuclei due to tooth extraction in C57BL/6J mice

Address all correspondence to:

Tetsuya Goto

Department of Oral Anatomy and Cell Biology, Kagoshima University Graduate School of Medical and Dental Sciences,

8-35-1 Sakuragaoka, Kagoshima 890-8544, Japan

E-mail: tgoto@dent.kagoshima-u.ac.jp

Abstract

The trigeminal mesencephalic nucleus (Vmes) is involved in reflex proprioception of the periodontium and masticatory muscle function. We evaluated the effects of tooth loss on neurodegeneration of the Vmes and trigeminal motor nucleus (Vmo). Bilateral maxillary molars of 8-week-old C57BL/6J mice were extracted under anesthesia. Fluoro-Gold (FG) was retrogradely injected into the extraction sockets and masticatory muscle, and the Vmes was labeled with adeno-associated virus encoding green fluorescent protein (AAV-GFP) for anterograde labeling. After tooth extraction, sections were generated and immunohistochemically stained using antibodies against Piezo2, ATF3, cleaved caspase-3, and TDP-43. Neural projections of the Vmes to the periodontium were confirmed via FG and AAV-GFP labeling. At 1 month after tooth extraction, a significant decrease in the number of Piezo2-immunoreactive (IR) Vmes neurons was observed. ATF3-IR neurons were detected on day 5 after tooth extraction, and their number decreased on days 10 and 15. Dead cleaved caspase-3-IR neurons were found among Vmes nerve cells on days 7 and 12. In the Vmo, transient TDP-43 pathology appeared at 1 month after tooth extraction. These results indicate the existence of neural projections from the Vmes to the periodontium in mice, and that tooth loss induces the death of Vmes neurons followed by TDP-43 pathology in the Vmo. Therefore, tooth loss induces Vmes neuronal cell death, causing Vmo neurodegeneration and possibly affecting masticatory function.

Keywords: Trigeminal mesencephalic nucleus; Trigeminal motor nucleus; Degeneration; TDP-43; Tooth extraction; Mouse

I. Introduction

The mesencephalic trigeminal nucleus (Vmes) neuron is unique in the trigeminal nervous system, and the cell bodies of primary afferent neurons are in the brainstem, not the trigeminal ganglion [16]. Vmes neurons innervate muscle spindles of the masticatory muscle [1], Ruffini endings of the periodontal ligament (PDL) [7], and the dental pulp [2]. These projections implicate the Vmes in the control of mastication [3,31,32] and periodontal reflexes [19]. Approximately 20% of the Vmes neurons in cats [12,27] and approximately 10–15% in monkeys [14] have afferent connections to the periodontal mechanoreceptors; the remainder project to the jaw-closing muscles.

The functions of the teeth, including mastication and pronunciation, are crucial for life. The neurodegeneration caused by tooth loss is not well-understood. Loss of teeth causes damage to the sensory receptors of the pulp and the PDL [23]. Additionally, degeneration and death of Vmes neurons occurred after peripheral axotomy in rats [28] and following tooth extraction in cats [20]. Also, some Vmes neurons died after tooth extraction in mice with induced Alzheimer's disease (AD) [11]. However, whether death of Vmes neurons occurs after tooth extraction in wild-type mice is unknown.

Because the Vmes directly controls the function of trigeminal motor neurons, neurodegeneration of Vmes neurons caused by tooth extraction may affect the trigeminal motor nucleus (Vmo). Transactivation responsive region-DNA-binding protein of 43 kDa (TDP-43) is an indicator of motor neuronal degeneration. In amyotrophic lateral sclerosis (ALS) [26] and frontotemporal dementia [4], TDP-43 reportedly translocates from the nucleus into the cytoplasm of motor neurons. In this study, we investigated whether TDP-43 neuropathology in Vmo neurons is caused by neurodegeneration of the Vmes after tooth extraction.

Here, we investigated the neuronal connection between Vmes neurons and Ruffini endings in the PDL in mice and evaluated the neurodegeneration and death of Vmes neurons following extraction of maxillary molars in C57BL/6J mice. We also examined TDP-43 pathology in Vmo neurons after tooth extraction. The findings indicate that tooth loss induces Vmes neuronal cell death, causing Vmo neurodegeneration and possibly affecting masticatory function.

II. Materials and Method

Animals

Forty-seven C57BL/6J (wild type, 25–30 g) male mice were used in this study. The mice were housed in cages at a constant temperature of 25℃ under a 12-h light-dark cycle (light from 6.00 to 18.00). This study was conducted in accordance with the appropriate animal protection guidelines and was approved by the Committee for Animal Experiments of Kagoshima University (approval number, D 20007, D200016). All procedures are in accordance with the ARRIVE guidelines and are carried out in accordance with the EC Directive 86/609/EEC for animal experiments. For tooth extraction, mice were deeply anesthetized with a combination anesthetic of medetomidine (0.15 mg/kg; Kobayashi Kako, Fukui, Japan), midazolam (2 mg/kg; Astellas Pharma, Tokyo, Japan), and butorphanol (2.5 mg/kg; Meiji Seika Pharma Co., Ltd., Tokyo, Japan) [15]. The mice were euthanized by deep anesthesia with sodium pentobarbital (75 mg/kg body weight) and transcardially perfused with 50 mL of phosphate-buffered saline (PBS; pH 7.3), followed by 100 mL of 4% paraformaldehyde, 75% saturated picric acid, and 0.1 M Na_2HPO_4 (adjusted to pH 7.0 with NaOH). The brains were next removed from the mice and postfixed with the same fixative for 4 h at 24°C. After cryoprotection in 30% sucrose in PBS, the brainstems were

cut on a cryostat, divided into 13 blocks containing six adjacent series of 50 μm sections from the rostral side to the caudal side of the Vmes, and stored at 4°C in PBS.

Retrograde and anterograde tracers

After tooth extraction, a 4% solution of FG (2-hydroxy-4, 4′-diamidinostilbene; Fluorochrome Inc., Denver, CO) in 0.9% saline was injected into the extracted tooth socket for retrograde tracing. For anterograde tracing, AAV2/1-CAG-Flex-eGFP (AV-1-ALL854) and AAV2/1-hSyn-Cre (AV-1-PV2676) were purchased from the Penn Vector Core, University of Pennsylvania. The two virus solutions were mixed and diluted to a final titer of 1×10^{11} genome copies/mL (GC/mL) for injection.

Surgery

The animals were deeply anesthetized with medetomidine (0.3 mg/kg), butorphanol (5.0 mg/kg), midazolam (4.0 mg/kg), and saline (1%) with intraperitoneal atipamezole (b.w/mouse) as an antagonist at 30 min after surgery. The anesthetized animals were mounted onto a stereotaxic apparatus (SR-5R; Narishige, Tokyo, Japan). For anterograde labeling of Vmes neurons, a mixture of AAV2/1-CAG-Flex-eGFP and AAV2/1-hSyn-Cre in 0.2 μL of 10 mM 0.9% sodium PBS (pH 7.4) was pressure injected into the Vmes (5.4 mm posterior to the bregma, 1.0 mm lateral to the midline, and 2.6 mm deep from the brain

surface) through a glass micropipette attached to a Pneumatic Pico Pump PV830 (World Precision Instruments, Sarasota, FL). Virus-injected mice survived for 2 weeks after the injection.

The bi-maxillary first to third molars in anesthetized mice were extracted using a dental probe. After the extraction, the mice were provided nutrient-rich food. Measurements of body weight were continued until 1 month after tooth extraction, when the mice began to appear normal.

Immunostaining

Brain sections were blocked with 3% donkey serum and 1% bovine serum albumin in Tris-buffered saline containing 0.1% TritonX-100. The primary antibodies were directed against ATF3 (1:1000; Abcam, Cambridge, UK), Piezo2 (1:1000; Novus Biologicals, Littleton, CO), active cleaved caspase-3 (1:100; Cell Signaling,_Danvers, MA), and TDP-43 (1:500; Proteintech, Chicago, IL).

For immunofluorescence, the sections were incubated overnight at 4°C with primary antibodies in PBS containing 0.3% Triton X-100, 0.12% lambda-carrageenan, and 1% donkey serum (PBS-XCD) and subsequently, for 4 h with 1 mg/mL Alexa Fluor 647-, 555-, or 488-conjugated goat anti-mouse or anti-rabbit antibody (1:1000; Thermo Fisher Scientific, Waltham, MA) in PBS-XCD. All incubations were performed at 24°C and were followed by rinsing with PBS containing 0.3% Triton X-100. The sections were observed under a confocal laser scanning microscope (LSM700; Zeiss, Oberkochen, Germany) or a

Nikon Eclipse E800M microscope (Nikon, Tokyo, Japan) equipped with a COMOS MP-102300A digital camera (Bio Tools Inc., Gunma, Japan) using ToupView software (ToupTek Photonics, Hangzhou, China).

For immunoperoxidase staining, the sections were incubated with an anti-cleaved caspase-3 antibody (1:100; Cell Signaling) overnight, biotinylated goat anti-rabbit immunoglobin G (1:200; Vector Labs, Burlington, CA) in PBS-XCD for 3 h, and avidin-biotin-peroxidase complex (1:100, elite variety; Vector Labs) in PBS-XCD for 1 h. Finally, the sections were incubated in 0.02% diaminobenzidine tetrahydrochloride and 0.005% H_2O_2 in 0.05 M Tris-HCl buffer (pH 7.6) for 10 min. The sections were mounted on glass slides and observed under a BX51 microscope (Olympus, Tokyo, Japan) equipped with a DP25 camera and cellSens software (Olympus).

Statistical analysis

Numerical values and error bars represent the means ± standard deviations. Mean values were compared using the unpaired Student's *t*-test or two-way analysis of variance followed by the Tukey *post hoc* test with R software (R Core Development Team, 2020).

III. Results

Characteristics of Vmes neurons projecting to the periodontal ligament

We investigated whether Vmes neurons project to the PDL of the upper molars by means of retrograde Fluoro-Gold (FG) and anterograde adeno-associated virus encoding green fluorescent protein (AAV-GFP) injection. Immediately following extraction of the upper molars and socket hemostasis, FG was dripped into the sockets. The mice were anesthetized, their heads were fixed to the device, and AAV-GFP was injected anterogradely at the location of the Vmes (Fig. 1A). FG-labelled Vmes neurons could be recognized at 5 days after FG injection (Fig. 1B) and remained evident at 10 and 15 days after injection (Fig. 1C, D). At 10 days after its injection into the Vmes, the localization of AAV-GFP was examined. AAV-GFP labeling was confirmed at a position neuroanatomically considered to be the Vmes in a brainstem tissue section (Fig. 1E). Moreover, AAV-GFP labeling was detected in the axon, and a structure thought to be a Ruffini ending was evident in the PDL of a mouse with confirmed AAV-GFP labeling of the Vmes (Fig. 1F, G).

There are morphological differences between Vmes neurons projecting to the PDL and those projecting to the muscle spindle of the masticatory muscle in cats [31,32]. We injected FG into the extraction socket and masseter muscle and assessed the diameter of the central cross-section of the Vmes neurons (Fig. 2A, B). We also measured the diameter of the central cross-section using confocal microscopy. Vmes neurons projecting to the PDL were significantly smaller than those projecting to the muscle spindle of the masticatory muscles (Fig. 2C).

Loss of Vmes neurons after tooth extraction

At 1 month after tooth extraction, we enumerated Piezo2-immunoreactive (IR) Vmes neurons in a section from each block (Fig. 3A). Control specimens were obtained from age-matched (3-month-old) mice that did not undergo tooth extraction. The Vmes was divided into 13 equal-size blocks along the rostro-caudal axis, and the number of Piezo2-IR Vmes neurons in one section of each block was determined (Fig. 3A–C). There were 24% fewer Piezo2-IR Vmes neurons in blocks 9–11 (Fig. 3D), and the number of Vmes neurons differed significantly between the control and extraction groups (unpaired *t*-test, $p = 0.005$; Fig. 3E).

Neurodegeneration of Vmes neurons after tooth extraction

Next, we investigated the post-extraction timings of Vmes neuronal damage and death using ATF3 for one section from block 11 and cleaved caspase-3 for all blocks. ATF3-IR nuclei became evident in Vmes neurons at 5 days after tooth extraction (Fig. 4A), and the number of ATF3-IR Vmes neurons decreased at 10 and 15 days after tooth extraction (Fig. 4B,C). Also, the number of ATF3-IR Vmes neurons was significantly reduced in the 5-day group compared to the 10-day group (unpaired *t*-test, $p = 0.008$. Fig. 4D). To confirm that neuronal death occurred at 5 to 10 days after tooth extraction, the number of cleaved caspase-3-IR Vmes neurons was examined. Cleaved caspase-3-IR Vmes neurons were detected in rostral and caudal sections (Fig. 4E, F). The number of cleaved caspase-3-IR

Vmes neurons was greater on day 7 after tooth extraction than on day 12, and a large number of cleaved caspase-3-IR neurons were observed in blocks 7–11 (Fig. 4G).

Effects on TDP-43 pathology after tooth extraction

Because Vmes neurons are involved in controlling the trigeminal motor nucleus, we examined the effects of tooth extraction on Vmo neurons using TDP-43 pathology as an indicator. Labeling with AAV-GFP confirmed that the axons of Vmes neurons reached the motor nucleus (Fig. 5A). Additional staining for acetylcholine transferase (ChAT), a marker of motor neurons, confirmed that the axons of Vmes neurons were in contact with Vmo neurons (Fig. 5B). TDP-43 pathology in the Vmo neurons after tooth extraction was examined by double staining using anti-ChAT and anti-TDP-43 antibodies (Fig. 5C–E). We identified three types of TDP-43 pathology: normal, pathological, and intermediate (Fig. 5F–K). In the normal type, TDP-43-IR stain was distributed throughout the nucleus. In the pathological type, TDP-43-IR stain was translocated from the nucleus to the cytoplasm, whereas in the intermediate type, some TDP-43-IR stained remained in the nucleus (Fig. 5H, K). We evaluated the frequency of each type at 1 and 2 months after tooth extraction (Fig. 5L). In the 2-month control, approximately 90% of the Vmo neurons were of the normal type, but some were of the intermediate (6.8%) and pathological (3.5%) types. At 1 month after tooth extraction, the frequency of the pathological type increased significantly to 14.9% (Tukey *post hoc* test, $p = 0.04$ *vs*. control). At 2 months after tooth

extraction, the frequency of the intermediate type also increased significantly (Tukey *post hoc* test, $p = 0.004$ *vs*. control) but that of the pathological type decreased to 5.7%.

IV. Discussion

Neuronal projections of Vmes neurons were associated with Ruffini ending-like structures in the PDL of C57BL/6J mice, and death of Vmes neurons was induced after extraction of maxillary molars. Neurodegeneration of Vmes neurons occurred within 5 days of tooth extraction and was followed by their death. Also, the cell death effects as observed in the Vmes extended to the Vmo, with pathological changes in TDP-43 distribution observed in the Vmo at 1 month after tooth extraction. Therefore, tooth extraction causes pathological changes in the Vmo.

The Vmes regulates jaw movements and is the only sensory nerve in the trigeminal nervous system that has primary neurons in the brain stem. In rats [6,7,17], cats [7] and monkeys [14], Vmes neurons have periodontal mechanoreceptor afferents. In this study, we examined Vmes-PDL mechanoreceptors in wild-type (C57BL/6J) mice using anterograde and retrograde labeling. Although Ruffini nerve endings are present in the mouse PDL [24,29], whether they contact the Vmes was unclear. From anterograde tracing using AAV-GFP, we found that Vmes neurons project to Ruffini nerve ending-like structures in the PDL of mice. Regarding retrograde tracing, because we extracted the molars without leaving the roots *in situ*, the Vmes could be accurately marked by dropping FG into the extraction socket.

Because the Vmes innervates at least two major regions—namely, the muscle spindle of the masticatory muscles and the PDL, we examined the size of the Vmes soma. We found that the Vmes is composed of two subpopulations of neurons—smaller Vmes neurons (20.02 ± 3.86 μm) innervate the PDL mechanoreceptor and larger Vmes neurons (23.51 ± 3.48 μm) innervate the masticatory muscle spindle. The Vmes in cats and rats can be divided into two subpopulations according to size. In rats, the larger Vmes has a diameter of 30–55 μm and the smaller, a diameter of ≤ 25 μm [21,22]. This difference in Vmes size is reportedly due to differences between pseudo-unipolar and multipolar neurons [22]. However, in this study, the size of the Vmes differed depending on whether their neurons innervated muscle spindles or the periodontal membrane.

Death of Vmes neurons after tooth extraction has been reported in 3xTg-AD model mice [11]. Because intense deposition of amyloid β occurs in the Vmes of 3xTg-AD mice, it is possible that amyloid β affects neuronal death in the Vmes. Using wild-type C57BL/6J mice, we observed similar neuronal death in the Vmes after extraction of the upper molars. Typically, even if a portion of the axons of peripheral neurons is damaged, Wallerian degeneration occurs, but neuronal death is rare. Although we do not know why tooth extraction causes neuronal cell death in the Vmes, the Vmes neuron is the only neuron with a soma localized in the brainstem; thus, damage to the axon terminal may also cause damage in the cell soma in the brainstem. Therefore, tooth extraction could cause degeneration of the entire nerve.

The number of ATF3-IR neurons in the Vmes region increased in a time-dependent manner, and cleaved caspase-3 positivity indicated neuronal death in the Vmes. In rats,

ATF3-IR staining was observed in the neurons of the trigeminal ganglion at 3 days after extraction of molars [13]. In this study, we found ATF3-IR Vmes neurons at 2 weeks after the extraction of maxillary molars from AD model mice [11]. ATF3-IR neurons appeared at 5 days after tooth extraction, and their number decreased at 10 and 15 days after tooth extraction. The decreased number of ATF3-IR cells could be due to cell death or recovery from damage. Therefore, we confirmed cell death using an antibody against cleaved caspase-3. The changes in position and number of cleaved caspase-3-IR neurons were similar to those observed for the cells at each site (Fig. 3D). That is, the decrease in cell number was greater on the caudal side, where there were a large number of cleaved caspase-3-IR neurons. However, some cleaved caspase-3-IR neurons survived. Also, caspase-3 is reportedly activated during apoptosis, indicating a functional shift in Vmes cells rather than their impending death [10,18]. Vmes neurons relay proprioceptive sensory information from mechanoreceptors in the PDLs and spindles of the masticatory muscle, and this information is relayed primarily to the rostral end of the Vmes, nucleus supratrigeminalis, and trigeminal motor nucleus as well as for parvocellular reticular formation. These projections form the reflex circuits governing the jaw-jerk reflex and control the mechanics of mastication [5,9].

We confirmed the existence of projections from Vmes to Vmo neurons using AAV-GFP. This finding suggests that the death of Vmes neurons causes neurodegeneration in the Vmo. TDP-43 is the major component of the neuronal inclusions characteristic of ALS and frontotemporal dementia (FTD) with ubiquitin inclusions. Although TDP-43 was initially thought to be specific to ALS and frontotemporal lobar degeneration, TDP-43 pathology has been detected in a number of other neurodegenerative diseases. These include diseases

associated with tau pathology, including Guam–Parkinson dementia complex and AD [34]. TDP-43-IR neuronal cytoplasmic inclusions with a rounded, specular, or skein-type appearance were observed in motor neurons of the trigeminal or facial cranial nerve of one patient with FTD and in the spinal cord of three patients with FTD and motor neuron disease. The majority of studies on TDP-43 have focused on its abnormal distribution in disease states—TDP-43-positive inclusion bodies are present in up to 97% of patients with ALS [30]. TDP-43 pathology is infrequent (≤ 3%) in neurologically normal elderly individuals [25]. Interestingly, 10.2% of the motor neurons in wild-type mice exhibited TDP-43 pathology, the frequency of which increased to 18.4% and 14.7% at 1 and 2 months, respectively, after tooth extraction. The more severe TDP-43 pathology in mouse motor neurons compared to human elderly motor neurons under normal conditions might be due to species differences or to effects on responsiveness to neurodegeneration. In wild-type mice, TDP-43 pathology was not found in the motor nerve immediately after tooth extraction (data not shown) but was found in Vmo neurons at 1–2 months after extraction. This suggests that the effects of tooth extraction on Vmo neurons were due to not only muscle atrophy caused by loss of occlusion but also the effect of decreased input from the Vmes. Reversible induction of TDP-43 granules has been reported in traumatic brain injury [33] and our results suggest that TDP-43 pathology is a reversible change. Further studies are needed on the effects of TDP-43 pathology on masticatory movements.

We used C57BL/6J wild-type mice to investigate projections from the Vmes to the PDL and evaluated the effects of extraction of maxillary bilateral molars on the Vmes and Vmo. Projections from the Vmes to the PDL were confirmed using FG-retrograde and AVV-

GFP-anterograde tracing. Extraction of the maxillary bilateral molars reduced the number of Vmes neurons by 24%, but ATF3-IR neurons were detected in the Vmes within 5 days, followed by cleaved caspase-3-IR staining and cell death. After neuronal death in the Vmes, TDP-43 pathology in the Vmo was reversible. Therefore, after tooth extraction, neurodegeneration spreads from Vmes to Vmo neurons and may affect the function of the masticatory muscles.

References

1. Alvarado-Mallart, M.R., Batini, C., Buisseret-Delmas, C., Corvisier, J. (1975) Trigeminal representations of the masticatory and extraocular proprioceptors as revealed by horseradish peroxidase retrograde transport. *Exp. Brain Res*. 23, 167–179.
2. Amano, N., Yoshino, K., Andoh, S., Kawagishi, S. (1987) Representation of tooth pulp in the mesencephalic trigeminal nucleus and the trigeminal ganglion in the cat, as revealed by retrogradely transported horseradish peroxidase. *Neurosci. Lett*. 82, 127–132.

3. Appenteng, K., Donga, R., Williams, R.G. (1985) Morphological and electrophysiological determination of the projections of jaw-elevator muscle spindle afferents in rats. *J. Physiol*. 369, 93–113.
4. Arai, T., Hasegawa, M., Akiyama, H., Ikeda, K., Nonaka, T., Mori, H., Mann, D., Tsuchiya, K., Yoshida, M., Hashizume, Y., Oda, T. (2006) TDP-43 is a component of ubiquitin-positive tau-negative inclusions in frontotemporal lobar degeneration and amyotrophic lateral sclerosis. *Biochem. Biophys. Res. Commun*. 351, 602–611.
5. Bae, Y.C., Nakagawa, S., Yasuda, K., Yabuta, N.H., Yoshida, A., Pil, P.K., Moritani, M., Chen, K., Nagase, Y., Takemura, M., Shigenaga, Y. (1996) Electron microscopic observation of synaptic connections of jaw-muscle spindle and periodontal afferent terminals in the trigeminal motor and supratrigeminal nuclei in the cat. *J. Comp. Neurol*. 374, 421–435.
6. Byers MR. (1985) Sensory innervation of periodontal ligament of rat molars consists of unencapsulated Ruffini-like mechanoreceptors and free nerve endings. *J Comp Neurol*. 231(4):500-518.
7. Byers MR, O'Connor TA, Martin RF, Dong WK. (1986) Mesencephalic trigeminal sensory neurons of cat: axon pathways and structure of mechanoreceptive endings in periodontal ligament. *J. Comp. Neurol*. 250(2), 181–191.
8. Byers MR, Dong WK. (1989) Comparison of trigeminal receptor location and structure in the periodontal ligament of different types of teeth from the rat, cat, and monkey. *J Comp Neurol*. 279(1):117-27.

9. Copray JC, Ter Horst GJ, Liem RS, van Willigen JD. (1990) Neurotransmitters and neuropeptides within the mesencephalic trigeminal nucleus of the rat: an immunohistochemical analysis. *Neuroscience*. 37(2):399-411.
10. D'Amelio M, Cavallucci V, Middei S, Marchetti C, Pacioni S, Ferri A, Diamantini A, De Zio D, Carrara P, Battistini L, Moreno S, Bacci A, Ammassari-Teule M, Marie H, Cecconi F. (2011) Caspase-3 triggers early synaptic dysfunction in a mouse model of Alzheimer's disease. *Nat Neurosci*. 2011 Jan;14(1):69-76.
11. Goto T, Kuramoto E, Dhar A, Wang RP, Seki H, Iwai H, Yamanaka A, Matsumoto SE, Hara H, Michikawa M, Ohyagi Y, Leung WK, Chang RC. (2020) Neurodegeneration of Trigeminal Mesencephalic Neurons by the Tooth Loss Triggers the Progression of Alzheimer's Disease in 3×Tg-AD Model Mice. *J Alzheimers Dis*. 76(4):1443-1459.
12. Gottlieb, S., Taylor, A., Bosley, M.A. (1984) The distribution of afferent neurons in the mesencephalic nucleus of the fifth nerve in the cat. *J. Comp. Neurol*. 228, 273–283.
13. Gunjigake KK, Goto T, Nakao K, Kobayashi S, Yamaguchi K. (2009) Activation of satellite glial cells in rat trigeminal ganglion after upper molar extraction. *Acta Histochem Cytochem*.42(5):143-9.
14. Hassanali, J. (1997) Quantitative and somatotopic mapping of neurons in the trigeminal mesencephalic nucleus and ganglion innervating teeth in monkey and baboon. *Arch. Oral Biol*. 42, 673–682.

15. Kurihara Y, Takechi M, Kurosaki K, Kobayashi Y, Kurosaw T. (2013) Anesthetic effects of a mixture of medetomidine, midazolam and butorphanol in two strains of mice. *Exp Anim* 62: 173-180.

16. Lazarov, N.E. (2002) Comparative analysis of the chemical neuroanatomy of the mammalian trigeminal ganglion and mesencephalic trigeminal nucleus, *Progress in Neurobiology.*

17. Li J, Xiong KH, Li YQ, Kaneko T, Mizuno N. (2000) Serotonergic innervation of mesencephalic trigeminal nucleus neurons: a light and electron microscopic study in the rat. *Neurosci Res*. 37(2):127-40.

18. Li Z, Jo J, Jia JM, Lo SC, Whitcomb DJ, Jiao S, Cho K, Sheng M. (2010) Caspase-3 activation via mitochondria is required for long-term depression and AMPA receptor internalization. *Cell*. 2010 May 28;141(5):859-71.

19. Lidsky, T.I., Labuszewski, T., Avitable, M.J., Robinson, J.H. (1979) The effects of stimulation of trigeminal sensory afferents upon caudate units in cats. *Brain Res. Bull*. 4, 9–14.

20. Linden, R.W., Scott, B.J. (1989) The effect of tooth extraction on periodontal ligament mechanoreceptors represented in the mesencephalic nucleus of the cat. *Arch. Oral Biol.* 34, 937–941.

21. Luo PF, Wang BR, Peng ZZ, Li JS. (1991) Morphological characteristics and terminating patterns of masseteric neurons of the mesencephalic trigeminal nucleus in the rat: an intracellular horseradish peroxidase labeling study. *J Comp Neurol*. 303(2):286-99.

22. Mineff EM, Popratiloff A, Usunoff KG, Marani E. (1998) Immunocytochemical localization of the AMPA receptor subunits in the mesencephalic trigeminal nucleus of the rat. *Arch Physiol Biochem*.106(3):203-9.

23. Muramoto, T., Takano, Y., Soma, K. (2000) Time-related changes in periodontal mechanoreceptors in rat molars after the loss of occlusal stimuli. *Arch. Histol. Cytol*. 63, 369–380.

24. Nagahama SI, Cunningham ML, Lee MY, Byers MR. (1998) Normal development of dental innervation and nerve/tissue interactions in the colony-stimulating factor-1 deficient osteopetrotic mouse. *Dev Dyn*. 211(1):52-9.

25. Nakashima-Yasuda H, Uryu K, Robinson J, Xie SX, Hurtig H, Duda JE, Arnold SE, Siderowf A, Grossman M, Leverenz JB, Woltjer R, Lopez OL, Hamilton R, Tsuang DW, Galasko D, Masliah E, Kaye J, Clark CM, Montine TJ, Lee VM, Trojanowski JQ. (2007) Co-morbidity of TDP-43 proteinopathy in Lewy body related diseases. *Acta Neuropathol*. 114(3):221-9.

26. Neumann, M., Sampathu, D.M., Kwong, L.K., Truax, A.C., Micsenyi, M.C., Chou, T.T., Bruce, J., Schuck, T., Grossman, M., Clark, C.M., McCluskey, L.F., Miller, B.L., Masliah, E., Mackenzie, I.R., Feldman, H., Feiden, W., Kretzschmar, H.A., Trojanowski, J.Q., Lee, V.M.Y. (2006) Ubiquitinated TDP-43 in frontotemporal lobar degeneration and amyotrophic lateral sclerosis. *Science*. 314, 130–133.

27. Nomura, S., Mizuno, N. (1985) Differential distribution of cell bodies and central axons of mesencephalic trigeminal nucleus neurons supplying the jaw-closing muscles and periodontal tissue: A transganglionic tracer study in the cat. *Brain Res*. 359, 311–319.

28. Raappana, P., Arvidsson, J. (1992) The reaction of mesencephalic trigeminal neurons to peripheral nerve transection in the adult rat. *Exp. brain Res*. 90, 567–571.

29. Piyapattamin T., Takano Y, Eto K, Soma K. (1999) Morphological changes in periodontal mechanoreceptors of mouse maxillary incisors after the experimental induction of anterior crossbite: a light and electron microscopic observation using immunohistochemistry for PGP 9.5. *Eur J Orthod*. 21(1):15-29.

30. Prasad A, Bharathi V, Sivalingam V, Girdhar A, Patel BK. (2019) Molecular Mechanisms of TDP-43 Misfolding and Pathology in Amyotrophic Lateral Sclerosis. *Front Mol Neurosci*. 2019 Feb 14;12:25.

31. Shigenaga, Y., Yoshida, A., Mitsuhiro, Y., Doe, K., Suemune, S. (1988a) Morphology of single mesencephalic trigeminal neurons innervating periodontal ligament of the cat. *Brain Res*. 448, 331–338.

32. Shigenaga, Y., Mitsuhiro, Y., Yoshida, A., Cao, C.Q., Tsuru, H. (1988b) Morphology of single mesencephalic trigeminal neurons innervating masseter muscle of the cat. *Brain Res*. 445, 392–399.

33. Wiesner D, Tar L, Linkus B, Chandrasekar A, Olde Heuvel F, Dupuis L, Tsao W, Wong PC, Ludolph A, Roselli F. (2018) Reversible induction of TDP-43 granules in cortical neurons after traumatic injury. *Exp Neurol*. Jan;299(Pt A):15-25.

34. Wilson AC, Dugger BN, Dickson DW, Wang DS. (2011) TDP-43 in aging and Alzheimer's disease - a review. *Int J Clin Exp Pathol*. 4(2):147-55.

Figure Legends

Figure. 1

Retrograde Fluoro-Gold (FG) and anterograde adeno-associated virus (AAV) encoding green fluorescent protein (GFP) injections were used to label neuronal connections. (A) (1) FG injection at the periodontal ligament (PDL) and (2) AAV-GFP injection at the trigeminal mesencephalic nucleus (Vmes). (B–D) Retrograde FG-labeled Vmes neurons at

5–15 days after injection. (E) GFP-labeled Vmes neurons (arrows). (F) GFP-labeled axon at the PDL and a higher-magnification view of the boxed area in (F). Arrowhead, axon; arrow, part of Ruffini ending. Scale bars: (B–D), 20 μm; (E), 50 μm; (F), 1 mm; (G), 300 μm.

Figure. 2

Difference in size of Vmes neurons projecting to the masticatory muscles (Mm) and PDL. (A, B) FG-labeled Vmes neurons connected to the Mm and PDL. (C) Mean size of Vmes neurons projecting to the Mm and PDL. Data are presented as the means ± standard deviations (SDs), n = 30. * $p < 0.05$, unpaired *t*-test.

Figure. 3.

Neuronal loss in the Vmes after tooth extraction. (A) The Vmes was divided into blocks along the rostral (1)-to-caudal (13) axis for histological analysis. (B, C) Immunocytochemical localization of Piezo2-immunoreactive (IR) Vmes neurons in caudal (right, block 11) regions in 3-month-old C57BL/6J mice without tooth extraction (B; Con, control) and with tooth extraction (C; Ext, 1 month after extraction). (D) Number of Vmes neurons in each block along the rostral (1)-to-caudal (14) axis of the Vmes in 3-month-old mice without tooth extraction (Con) and with tooth extraction (Ext). (E) Total number of Vmes neurons in 13 sections from mice in the Con and Ext groups. Data are presented as the means ± SDs, n = 10. * $p < 0.05$, unpaired *t*-test.

Figure. 4

Damaged and dead Vmes neurons after tooth extraction. (A–C) Damaged Vmes neurons as indicated by ATF3-IR positivity (arrows) in (A) (5 days), (B) (10 days), and (C) (15 days) after extraction of the maxillary molars. (D) Temporal changes in the number of ATF3-IR Vmes neurons in block #9. Data are presented as the means ± SDs, n = 10. * $p < 0.01$, unpaired *t*-test. (E, F) Dead Vmes neurons as indicated by cleaved caspase-3-IR positivity (arrows) at the rostral (F) and caudal (F) ends of the Vmes at 1 month after extraction. Scale bars: (C, E, F), 50 μm. (G) Number of cleaved caspase-3-IR neurons in each block along the rostral (2)-to-caudal (12) axis of the Vmes at 7 days (Ext 7d) and 12 days (Ext 12d) after tooth extraction. Data are presented as the means ± SDs, n = 10.

Figure. 5

Effects of tooth extraction on TDP-43 pathology in trigeminal motor neurons.
(A) AAV-GFP-labeled axons extending from Vmes neurons (arrowhead) to motor neurons. (B) Higher-magnification view of the boxed area in (A). Arrows indicate choline acetyltransferase (ChAT)-IR trigeminal motor (Vmo) neurons. ChAT-IR trigeminal neurons (C, F, I), immunoreactivity of TDP-43 (D, G, J), and merged images (E, H, K) of the Vmo at 1 month after extraction. (H): Double arrows, pathological-type TDP-43; arrow, normal-type TDP-43. (K, L): Arrowhead, intermediate-type TDP-43. Scale bars: (A), 100 μm; (B), 20 μm; (E), 30 μm; (H, K), 10 μm. (L) Distribution of normal-, intermediate-, and pathological-type TDP-43 in the Vmo. 2M Con, 2-month-old mice that did not undergo tooth extraction; 3M Ext 1M, 3-month-old mice at 1 month after tooth extraction; 4M Ext

2M, 4-month-old mice at 2 months after tooth extraction. Data are presented as the means ± SDs, n = 13. * $p < 0.05$, ** $p < 0.01$, vs controls, Tukey *post hoc* test.

Conflict of interest

The authors declare no conflicts of interest.

Authorship contribution statement

Ashis Dhar: Conceptualization - Data curation - Writing, **Eriko Kuramoto:** Methodology – Investigation – Resources - Funding acquisition, **Makoto Fukushima:** Investigation - Resources, **Haruki Iwai:** Investigation - Resources, **Atsushi Yamanaka :** Investigation - Resources, **Tetsuya Goto:** Conceptualization – Project administration - Funding acquisition - Data curation - Writing

Acknowledgements

This project was partially supported by Grant-in-Aid for Scientific Research (C) (20K10296 to Goto , 16K11454 to Kuramoto) from the Ministry of Education, Culture, Sports, Science and Technology, Japan.

Fig 1

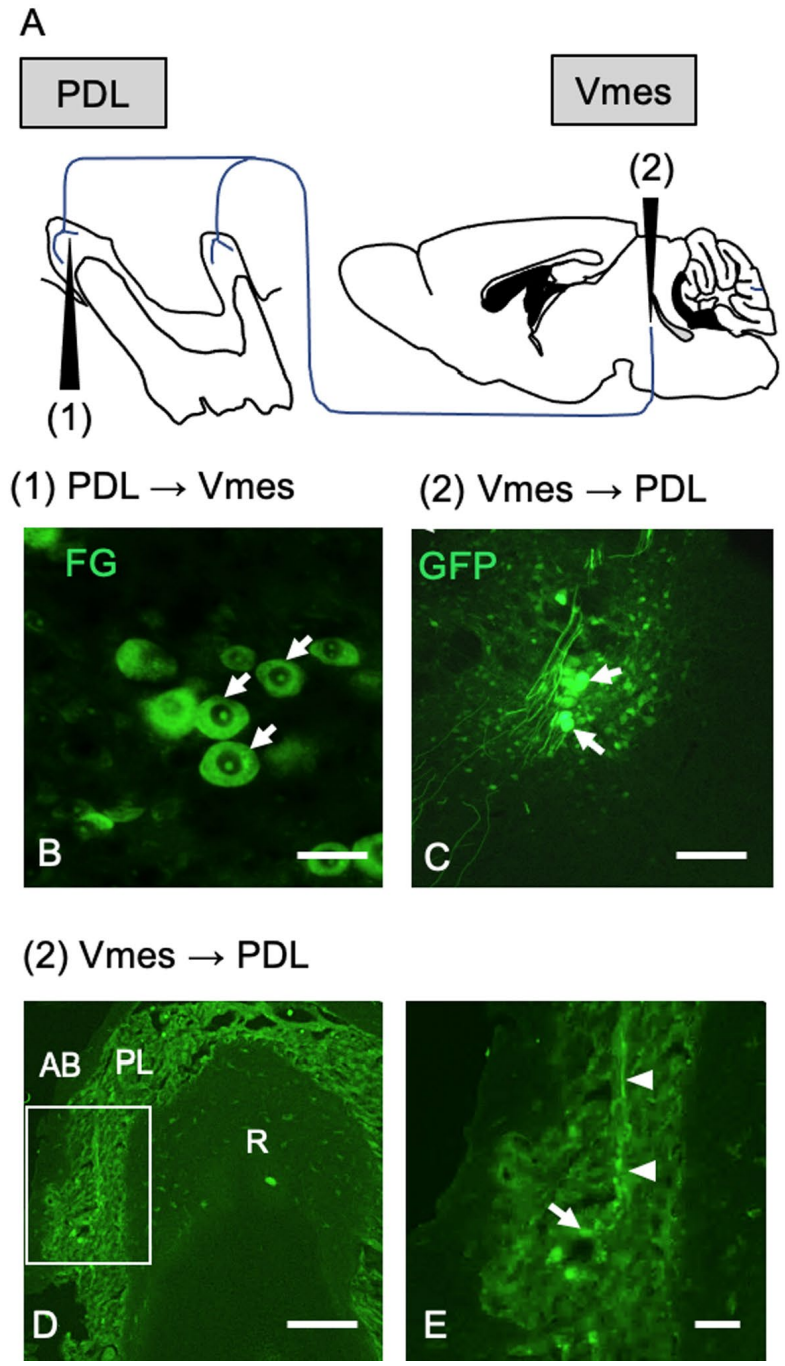

Fig 2

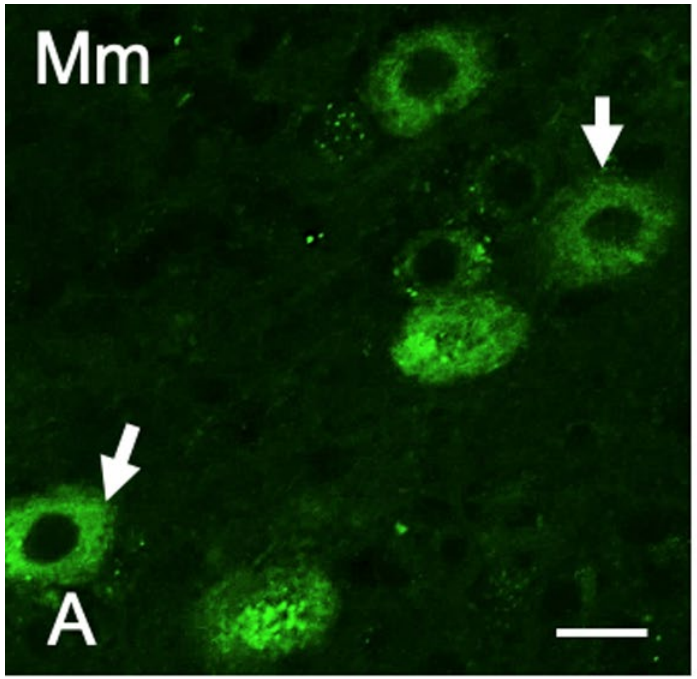

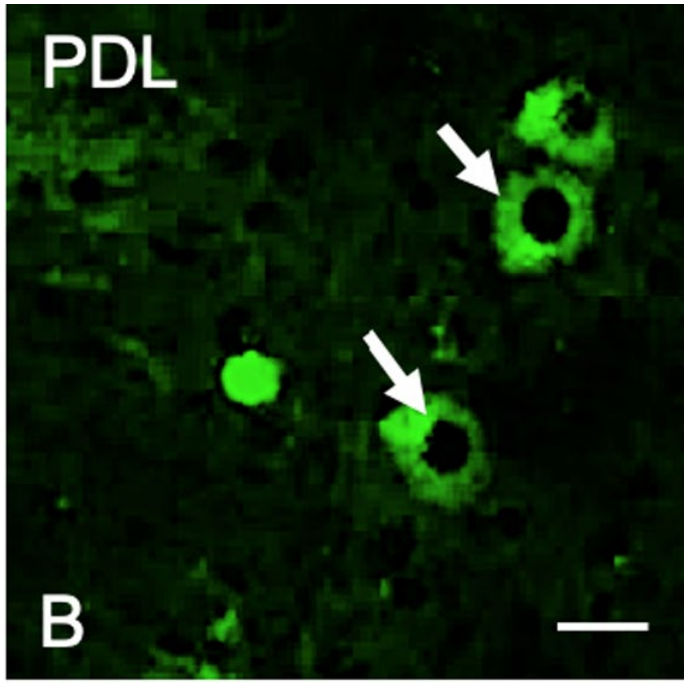

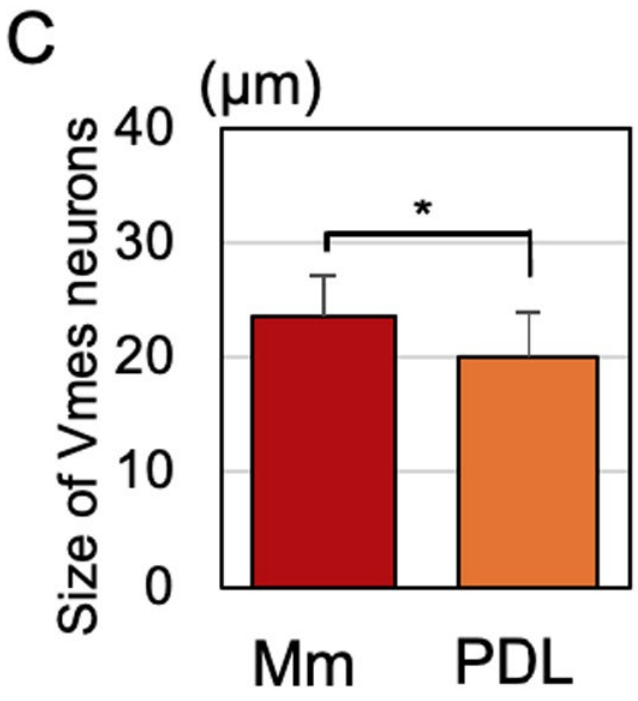

Fig 3

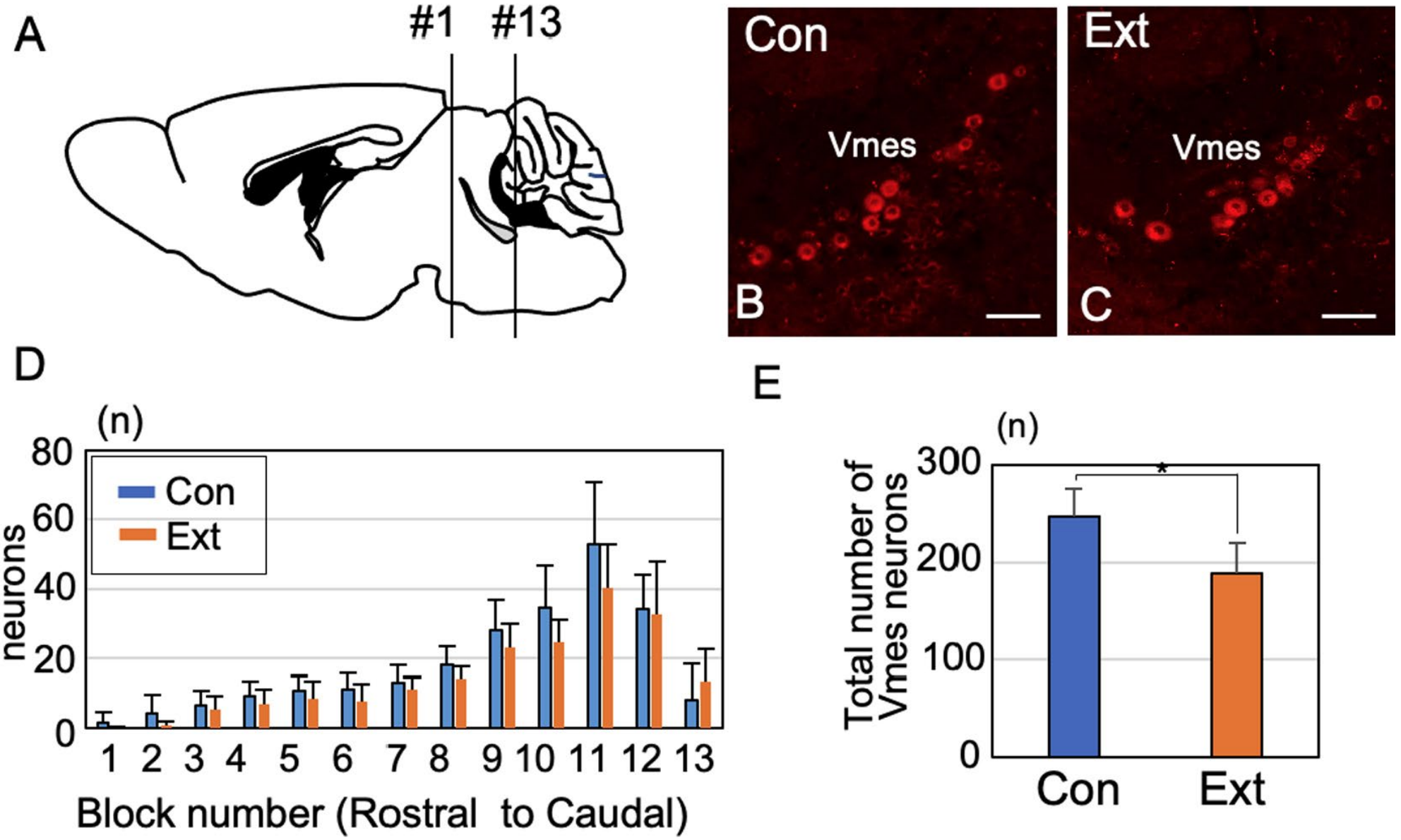
A
#1
#13
Con
Vmes
B
Ext
Vmes
C
D
(n)
Number of Vmes neurons
80
60
40
20
0
Con
Ext
1 2 3 4 5 6 7 8 9 10 11 12 13
Block number (Rostral to Caudal)
E
(n)
Total number of Vmes neurons
300
200
100
0
*
Con
Ext

Fig 4

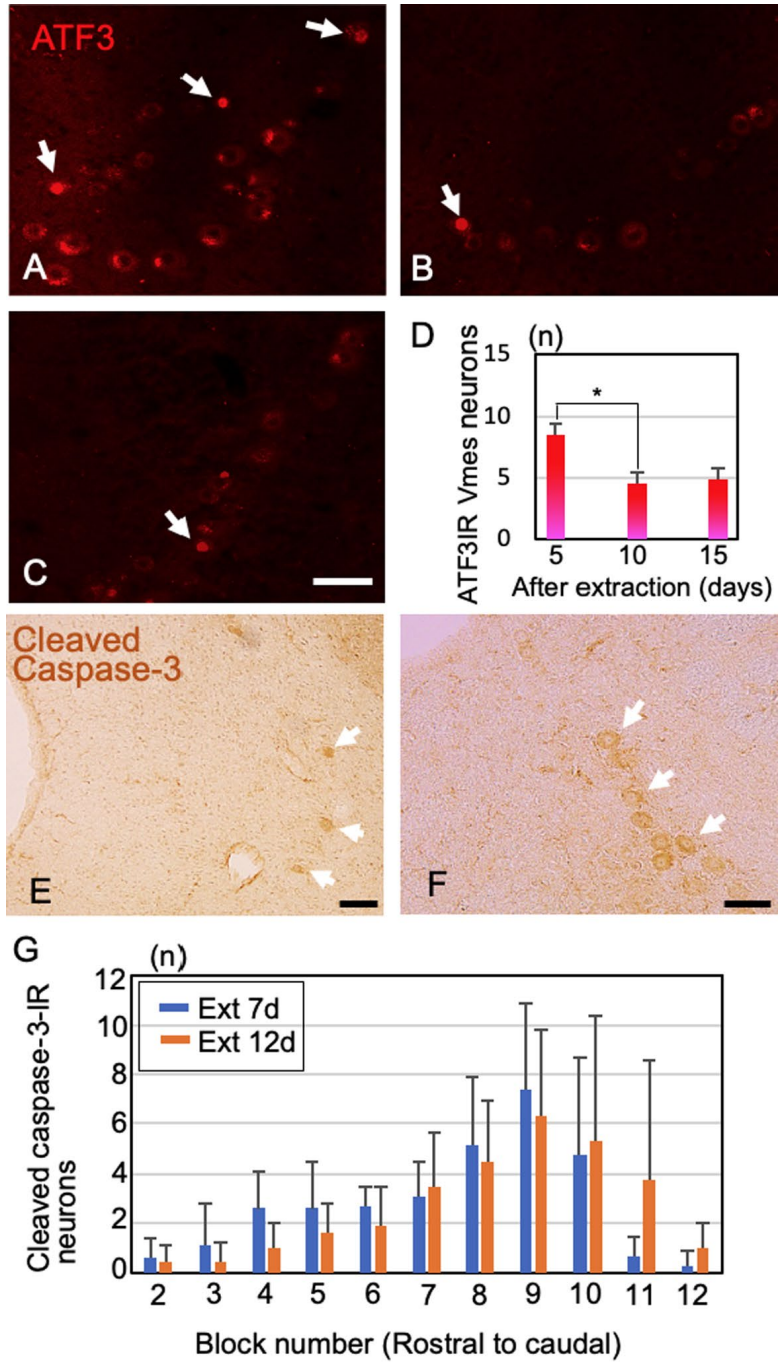
ATF3
A
B
C
D
(n)
ATF3IR Vmes neurons
15
10
5
0
*
5
10
15
After extraction (days)
Cleaved
Caspase-3
E
F
G
(n)
Ext 7d
Ext 12d
Cleaved caspase-3-IR
neurons
12
10
8
6
4
2
0
2
3
4
5
6
7
8
9
10
11
12
Block number (Rostral to caudal)

Fig 5

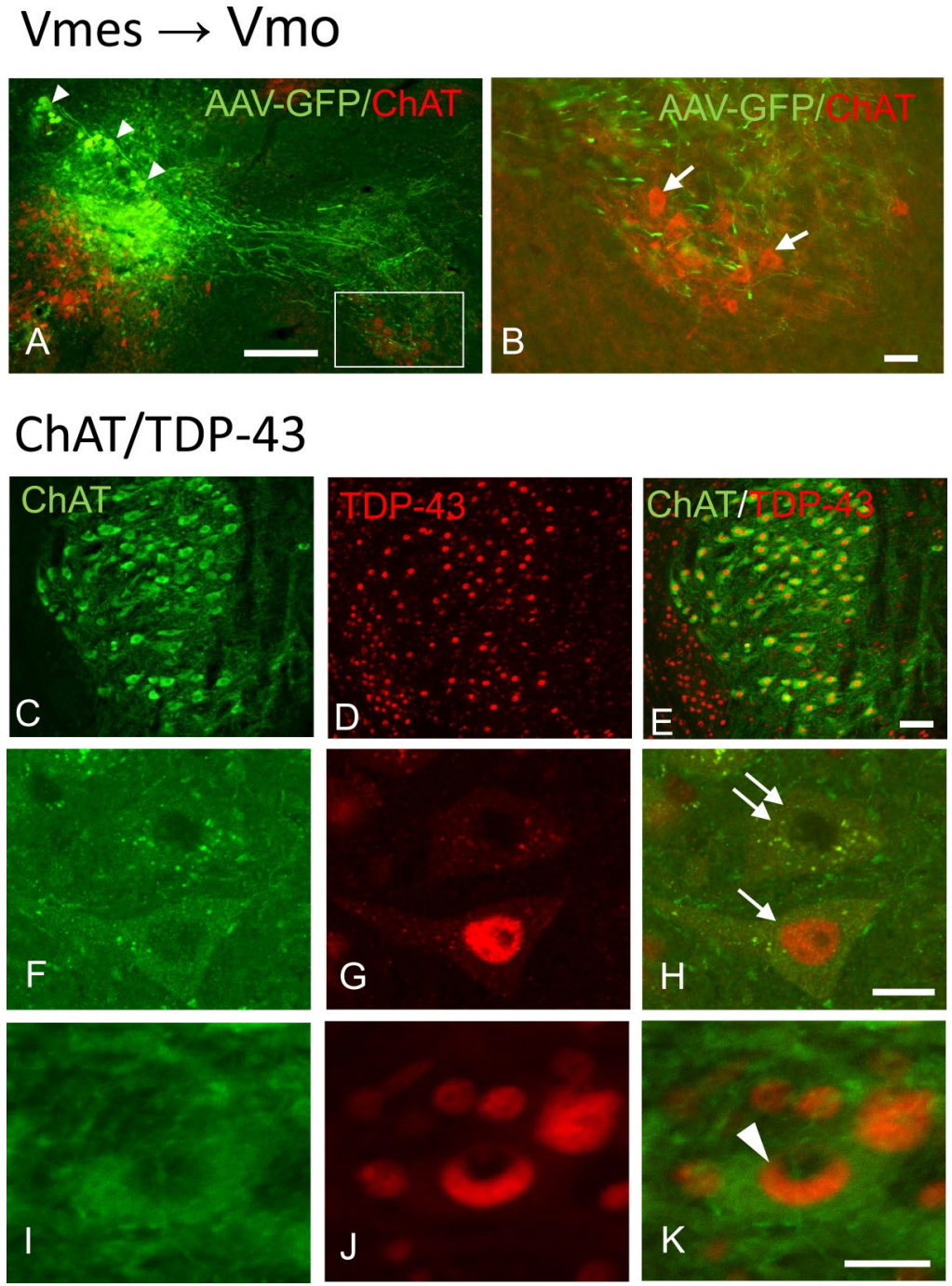
Vmes → Vmo
AAV-GFP/ChAT
A
AAV-GFP/ChAT
B
ChAT/TDP-43
ChAT
C
TDP-43
D
ChAT/TDP-43
E
F
G
H
I
J
K

Fig 6

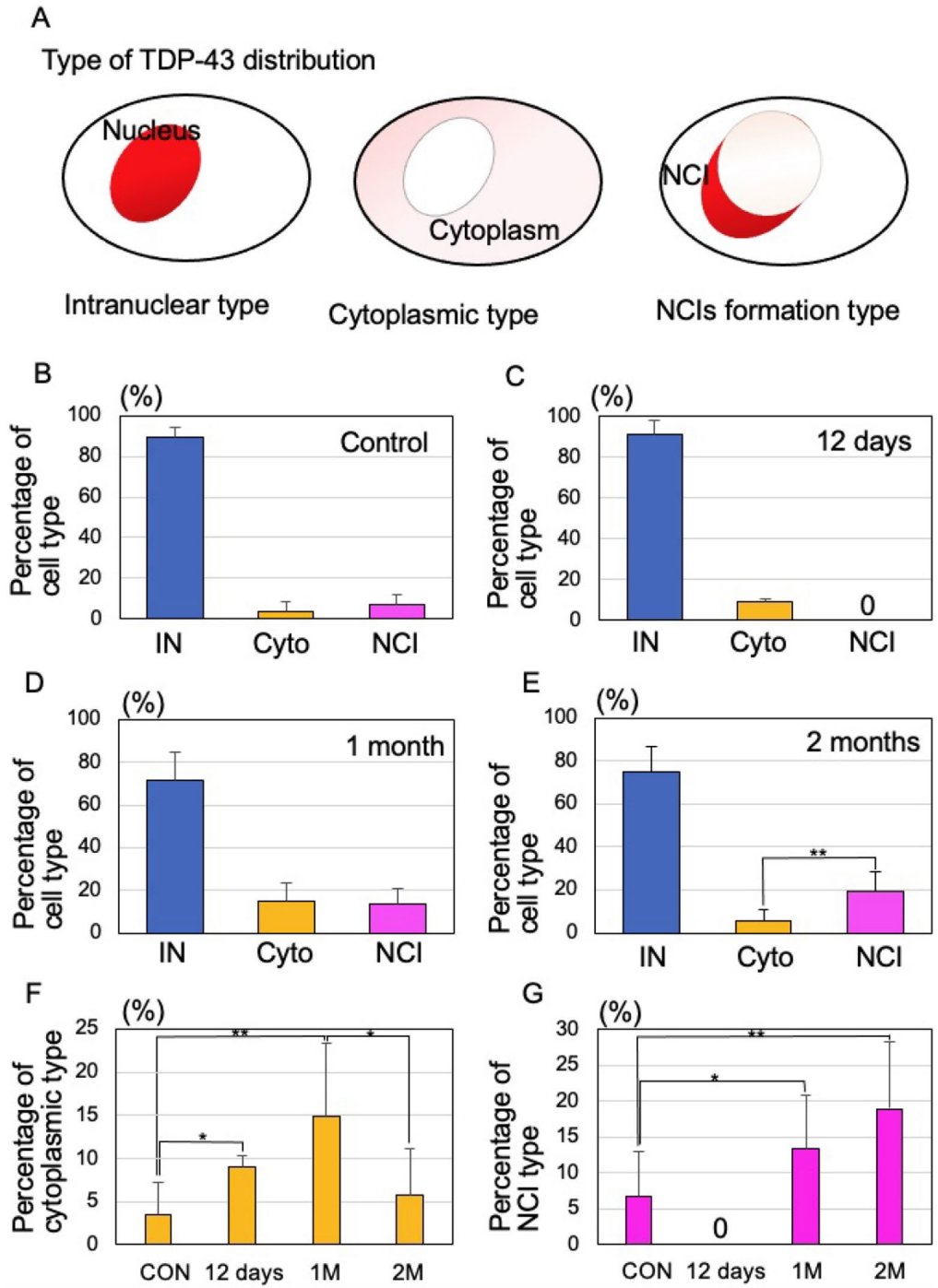
A
Type of TDP-43 distribution
Nucleus
Cytoplasm
NCI
Intranuclear type
Cytoplasmic type
NCIs formation type
B
(%)
Percentage of cell type
Control
IN
Cyto
NCI
C
12 days
0
D
1 month
E
2 months
**
F
Percentage of cytoplasmic type
*
CON
12 days
1M
2M
G
Percentage of NCI type